Advances in Materials Technology for Fossil Power Plants
Proceedings from the Eighth International Conference
October 11–14, 2016, Albufeira, Algarve, Portugal
https://doi.org/10.31399/asm.cp.am-epri-2016p0466

J. Parker, J. Shingledecker, J. Siefert, editors

EVALUATION OF LONG-TERM CREEP RUPTURE LIFE OF GR.91 STEEL BY ANALYSIS OF ON-GOING CREEP CURVES

Kouichi Maruyama, Junya Nakamura and Kyosuke Yoshimi
Tohoku University, 6-6-02 Aramaki-Aoba, Aoba-ku, Sendai, 980-8579, Japan

Yuji Nagae
Japan Atomic Energy Agency, 4002 Naritacho, Oharai, 319-1393, Japan

ABSTRACT

A methodology is developed for evaluating its creep rupture life from analysis of an on-going creep curve with the aid of an Ω creep curve equation. The method is applied to on-going creep curves of grade 91 steel for evaluating their rupture lives. Quick decrease in creep rupture strength has been reported recently in long-term creep of grade 91 steel. The quick decrease of the steel is discussed by using the rupture lives evaluated. The quick decrease is confirmed in the present study in the time range longer than $3x10^4$h at 600°C.
Keywords: Omega creep curve equation, Rupture life evaluation, Breakdown of creep strength

INTRODUCTION

Grade 91 steel (9Cr-1Mo-V-Nb steel, referred to as Gr.91 steel, hereafter) is one of the heat resistant steels most widely used in fossil fired electric power plants. The steel is used at temperatures from 550 to 600°C for 20 to 30 years. For safe operation of power boilers, we need creep rupture strength (stress that causes creep fracture at a given time) of the steel in the temperature and time ranges. Accelerated creep tests are necessary for evaluating the long-term creep rupture strength. The accelerated tests are usually performed at higher temperatures and higher stresses, and creep rupture lives obtained from the tests are formulated with a time-temperature parameter (TTP), such as Larson-Miller parameter. Then the formula is extrapolated to lower temperature for evaluating the long-term creep rupture strength. The parameters assume that temperature T dependence of creep rupture life t_r is unique in the whole data set to be formulated. However, in many materials slope of a $\ln t_r$ - $1/T$ curve changes to a gentle slope at lower temperatures. This change results in overestimation of long-term creep rupture life when the high temperature data are extrapolated to a low temperature without taking account of the change in slope [1-3]. The overestimation is especially substantial in creep strength enhanced ferritic steels [4-9].

Rupture life can also be evaluated from analysis of a creep curve. Suppose a creep test of Gr.91 steel is performed under a service condition of a plant component. Its minimum creep rate is reached around 25% of its rupture life [10]. Monkman-Grant relation [11] has been known between creep rupture life and minimum creep rate. Rupture life can be evaluated directly from the minimum creep rate without extrapolation to a lower temperature. However, it is not certain whether the exponent of Monkman-Grant relation is unchanged over a wide range of creep conditions [10,12]. Abe [10] has improved the Monkman-Grant relation by adding the slope, Ω = *d*ln(creep strain rate)/*d*(strain), in the tertiary creep stage to the relation. An Ω creep curve equation

[13] has been proposed to evaluate its rupture life by means of analysis of an on-going creep curve. The equation contains several parameters characterizing a creep curve. If the parameters can be determined at a certain point before creep fracture, its creep curve afterward and its rupture life can be evaluated by the creep curve equation with the parameters determined. This type of rupture life evaluation has not been fully developed yet. The present study focuses on the rupture life evaluation based on such a creep curve analysis.

The analysis of a creep curve needs a creep curve equation that can describe strain accumulation as a function of time. In order to choose a creep curve equation, characteristics of creep curves of Gr.91 steel should be made clear. The creep curve equation should be modified, so that it can describe both primary and tertiary creep stages. Methodology for evaluating rupture life from the information obtained from the creep curve analysis should be developed. These are the objectives of the present study. The analysis method of creep curve is applied to on-going creep curves of Gr.91 steel. Their current creep test durations are 166,600h (157MPa) and 145,700h (137MPa) at 550^{o}C. A thorough investigation on creep deformation behavior of Gr.91 steel have been reported recently by Abe [10]. The creep deformation behavior he reported is examined with creep curves of the present study. The present study includes longer creep curves than those reported by Abe [10] and in NIMS Creep Data Sheet [14,15].

Quick decrease in creep rupture strength occurs in long-term creep of Gr.91 steel [3,16]. The stress and rupture life ranges in which the quick strength decrease occurs is referred to as region L_2 in the present study. The region was first found in 2010 [16], and has been confirmed in 2016 [3]. Since plant components made of Gr.91 steel are used in region L_2, the region should be important from an engineering point of view. However, the region is not recognized widely. The presence of region L_2 is discussed on the basis of the long-term rupture lives evaluated in the present study.

MATERIALS

The present study analyzes creep curves of four heats of Gr.91 steel. Chemical compositions of major elements in each heat are listed in Table 1 together with their heat treatment procedures. Heats A to C were subjected to stress relief annealing after usual normalizing and tempering treatments. Heats C and CNT are the same material except for the stress relief annealing. Creep specimens were cut parallel to rolling direction from the center of plate products. Creep tests were performed in air under constant load.

Table 1: Chemical concentrations in mass% and heat treatments of four heats of Gr.91 steel studied.

Heat	C	Ni	Cr	Mo	V	Nb	Normalizing	Tempering
A	0.10	0.07	8.73	0.96	0.22	0.09	1050^{o}C, 50min	780^{o}C, 60min + 740^{o}C, 500min
B	0.10	0.06	8.75	0.97	0.21	0.089	1050^{o}C, 65min	780^{o}C, 85min + 740^{o}C, 640min
C	0.09	0.04	8.76	0.94	0.21	0.08	1060^{o}C, 60min	760^{o}C, 60min + 740^{o}C, 500min
CNT	0.09	0.04	8.76	0.94	0.21	0.08	1060^{o}C, 60min	760^{o}C, 60min

CREEP CURVE EQUATION

A creep curve equation is needed for formulating a creep curve. Since the objective of the present study is evaluation of creep rupture life, we need an equation that can describe the tertiary creep stage. Several creep curve equations for tertiary creep have been proposed so far. Representatives of such equations are a θ equation [17,18] and an Ω equation [19]. The equations assume the following relations for a tertiary creep cure, respectively:

$$\dot{\varepsilon} = \theta (\varepsilon - \varepsilon_o) \quad (1)$$

$$\ln \dot{\varepsilon} = \ln B + \Omega \varepsilon \quad (2)$$

where $\dot{\varepsilon}$ is the creep strain rate, ε is the creep strain, and θ, ε_o, B and Ω are parameters characterizing a tertiary creep curve. The former expects a linear relation to a $\dot{\varepsilon}$ vs ε curve when $\dot{\varepsilon}$ is taken for the ordinate, whereas the latter expects a linear line when $\log \dot{\varepsilon}$ is taken for the ordinate.

A creep curve of heat C tested at a high stress, 216MPa at 550°C, is drawn in Fig.1. The $\log \dot{\varepsilon}$ vs. ε curve in Fig.1 (b) approaches an asymptotic line after 6% strain, supporting the relation of Eq.(2). Such a linear relation of $\log \dot{\varepsilon}$ vs. ε curves in tertiary creep has been reported experimentally on creep strength enhanced ferritic steels [10,19,20]. Another creep curve of heat CNT tested at a low stress, 93MPa at 600°C, is drawn in the form of strain rate vs. strain in Fig.2. Rupture life of the test is 95,918h. At low stresses, $\log \dot{\varepsilon}$ vs. ε curves in the later stage of tertiary creep are not straight (see Fig.2 (a)); the slope decreases gradually with increasing strain, suggesting some deviation from the relation of Eq.(2). In order to examine the possibility of Eq.(1), the same curve is shown in Fig.2 (b) taking $\dot{\varepsilon}$ as the ordinate. The slope in the tertiary stage, however, increases monotonously with increasing strain, contrary to the expectation of Eq.(1). These findings suggest that the Ω creep curve equation is more suitable for formulating the tertiary creep curves of Gr.91 steel rather than the θ creep curve equation. The deviation from Eq.(2) at low stresses has been reported in other heats of Gr.91 steel [10,14,15]. The deviation should be kept in mind when evaluating rupture life.

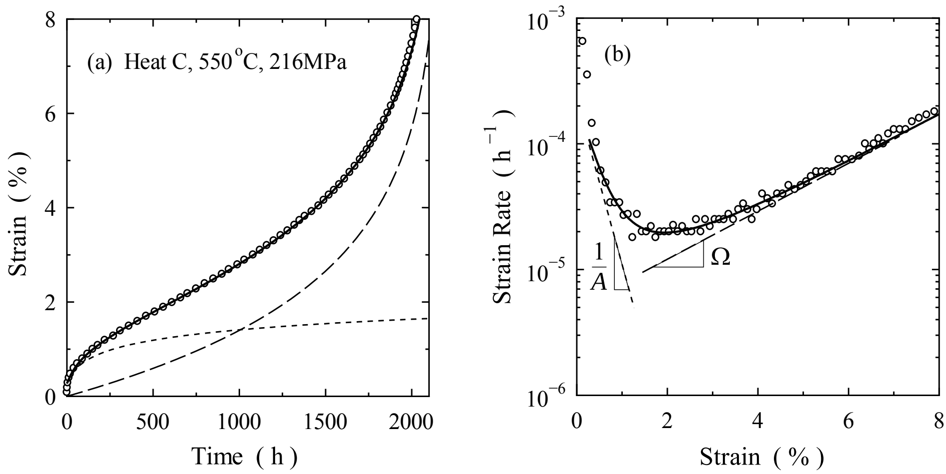

Figure 1: (a) A representative creep curve and (b) its corresponding strain rate vs. strain curve of heat C tested at 550°C under 216MPa. The solid curves were determined by curve fitting based on Eq.(3). The dotted and dashed curves represent the first and second terms and the third term of Eq.(3), respectively.

As evident in Figs.1 and 2, there is a pronounced primary creep stage in creep of Gr. 91 steel. Due to the contribution of the primary creep the slope $d\dot{\varepsilon}/d\varepsilon$ in Fig.1 (b) increases gradually to the asymptotic line describing the later stage of the tertiary creep. Therefore, a creep curve equation with a primary creep term is better in terms of formulation of a creep curve of Gr.91 steel than the one without the primary creep term. The former equation can predict rupture life with higher accuracy than the latter [19]. Taking account of the primary creep stage, let us use the following creep curve equation:

$$\varepsilon = \varepsilon_i + A \ln(1 + \alpha t) - (1/\Omega) \ln(1 - \beta t) \qquad (3)$$

$$\dot{\varepsilon} = \{\alpha A/(1 + \alpha t)\} + \{(\beta/\Omega)/(1 - \beta t)\} \qquad (4)$$

where t is the time, ε_i and A are constants, and α and β are rate constants. The second and third terms in Eq.(3) describe the primary creep and the tertiary creep, respectively. The parameters A and Ω correspond to the slopes of the asymptotic lines in the primary and tertiary stages, respectively (see Fig.1 (b)).

Maruyama *et al.* [19] have used a creep curve equation that is similar to Eq.(3) but assumes the same slopes of asymptotic lines both for the primary creep and the tertiary creep, namely $\Omega = 1/A$. On the other hand, Dewees and Hantz [21] have used an equation taking different slopes for the primary and tertiary creep stages. The latter equation is more general and more suitable to the present creep curves shown in Figs.1 and 2. Therefore, Eq.(3) is used in the present analyses of creep curves. The five parameters included in Eq.(3) are determined so that the equation gives the best fit to a creep strain vs. time curve measured experimentally. The solid curves in Figs.1 and 2 are creep curves and strain rate-strain curves calculated by Eq.(3) with the parameters. The curves can well represent the experimental results.

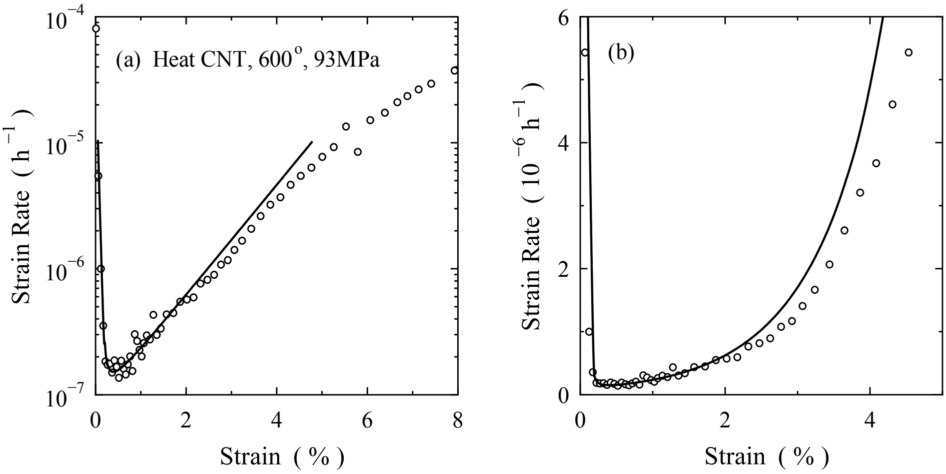

Figure 2: A creep strain rate vs. strain curve tested at 600°C under 93MPa. The ordinate is logarithmic and normal scales in (a) and (b), respectively. The solid curves are a regression curve determined with Eq.(3).

SHAPE OF CREEP CURVES

Primary Creep

Representative creep curves of the present steel are given in Figs.1 and 2. All of them are a typical classical creep curve: the creep rate decreases in the primary creep stage, takes a minimum and then increases to fracture in the tertiary creep stage. Strain to minimum creep rate ε_m is plotted in Fig.3 (a) as a function of creep testing stress. ε_m is about 2% and independent of stress at the high stresses of 550 and 600°C, but decreases with decreasing stress at the low stresses. The following relation is obtained from the data points tested in the low stress regions at 600 to 700°C:

$$\varepsilon_m = -5.35 + 0.276\,\sigma + 5390\,(1/T) \quad (5)$$

where σ and *T* are the creep testing stress and temperature, respectively. The dashed line at 550°C is calculated with this equation. The data points of the temperature tested at the low stresses coincide fairly well with the dashed line. The stress and temperature dependences of ε_m are similar to the ones reported by Abe [10] on Gr.91 steel.

The ratio of time to minimum creep rare t_m to rupture life t_r is shown in Fig.3 (b). Abe [10] has reported that an average value of t_m/t_r is 0.27 on Gr.91 steel. This is true in the present material: $t_m/t_r = 0.27$ at $\sigma > 110$MPa and = 0.23 at $\sigma < 110$MPa. However, the scatter in data points is very large as is the case in the literature [10]. Abe [10] has reported that the ratio t_m/t_r decreases with decreasing stress but is independent of creep temperature. He has proposed to evaluate rupture life from t_m based on the ratio. If we carefully look at Fig.3 (b), stress dependence of the ratio is represented by the dotted lines at each temperature. The ratio increases with decreasing stress at 550°C. At 600 it increases with decreasing stress at the higher stresses, but decreases with decreasing stress below 130MPa. At 650°C the ratio decreases with decreasing stress below 80MPa, but is independent of stress above the critical stress. The ratio increases with decreasing stress at 700°C. It seems hard to formulate the ratio as a function of stress and temperature.

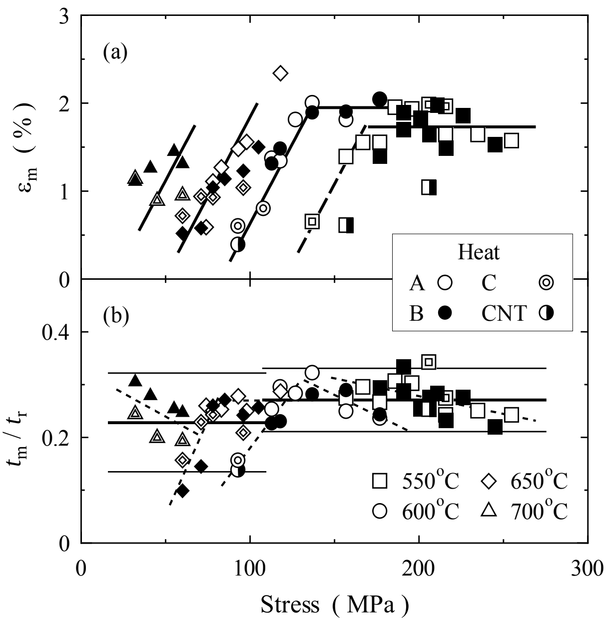

Figure 3: (a) Strain to minimum creep rate ε_m, and (b) ratio of time to minimum creep rate t_m to rupture life t_r plotted against creep testing stress.

Tertiary Creep

Representative creep curves of heat B are drawn in Fig.4 in the form of a $\log\dot{\varepsilon}$ vs. ε curve. They were creep tested at 600°C. Let us define the slope of a $\ln\dot{\varepsilon}$ vs. ε curve at a given strain as ω:

$$d\ln\dot{\varepsilon}/d\varepsilon = \omega \quad (6)$$

ω is negative in the primary creep stage, and increases with increasing strain. It becomes zero at the minimum creep rate, and increases to the slope of an asymptotic line, namely Ω of Eq.(3). The slope ω becomes independent of strain above 4% strain at the higher stresses (177 and 157MPa), but decreases with increasing strain above 4% strain at the lower stresses (137 and 118MPa as well as 93MPa in Fig.2). The slope ω for example at 4% strain increases with decreasing stress.

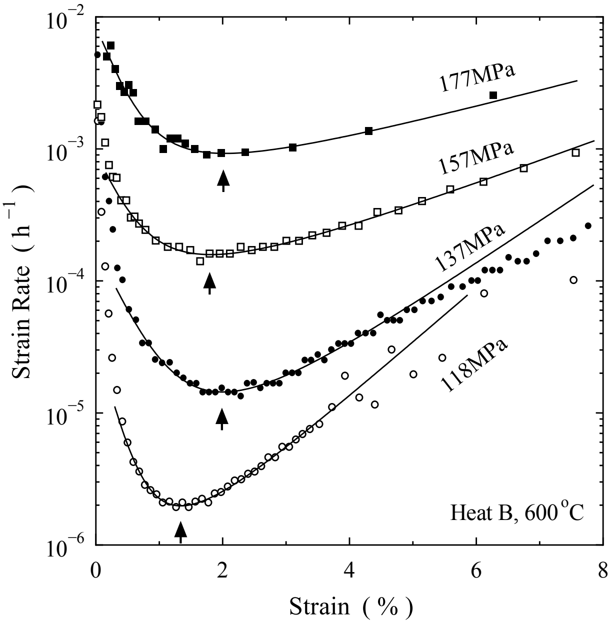

Figure 4: Representative creep curves of heat B tested at 600°C. The curves are shown in the form of creep strain rate vs. strain. The arrows indicate the point of minimum creep rate.

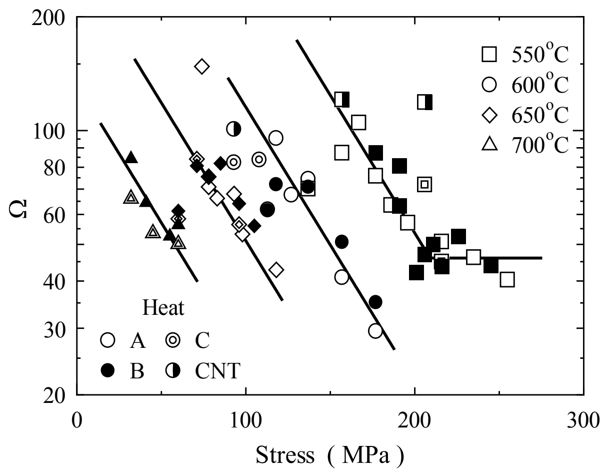

Figure 5: Stress dependence of Ω of Eq.(3).

The values of Ω in Eq.(3) are plotted against creep stress in Fig.5. The values were obtained from curve filling of Eq.(3) to each measured creep curve. In the case of Fig.1 (b), Ω is the slope $d\ln\dot{\varepsilon}/d\varepsilon$ of the asymptotic line. In the case of Fig.2 with the decrease of ω in the tertiary creep, Ω of Eq.(3) varies with creep curve data analyzed. In the analysis of the creep curve, data points above a critical strain ε_c are discarded in the curve fitting. The values of Ω increase with decreasing ε_c, and approach an upper limit value. The values of Ω in Fig.5 are such the steepest slope of asymptotic lines.

As evident at 550°C in Fig.5, Ω is independent of stress above 210MPa, and increases with decreasing stress below 210MPa. The stress insensitive region is not seen above 600°C in the present study. According to the NIMS Creep Data Sheet [14] Ω is almost the same at 160 and 200MPa at 600°C. This fact suggests that the stress insensitive Ω should appear at higher stresses even at 600°C. Ω increases from about 40 to above 100 with decreasing stress. Ω decreases with increasing temperature. These facts are essentially the same as the ones reported by Abe [10] on Gr.91 steel. The stress σ and temperature *T* dependence of Ω is expressed as follows:

$$\Omega = 1.85\text{x}10^{-4} \exp(-0.0168\ \sigma) \exp(109[\text{kJ/mol}]/R\ T) \quad (7)$$

where *R* is the gas constant. It is not clear whether there is an upper limit of Ω at further lower stresses.

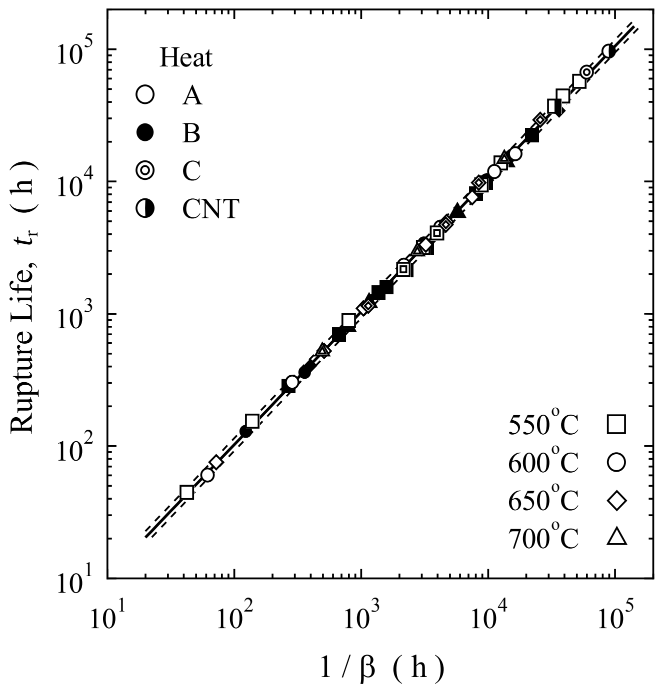

Figure 6: Correlation between actual rupture life t_r and estimated one, 1/β.

Grade 91 steel has a tempered martensite lath microstructure consisting of fine and elongated subgrains. Since the fine subgrains are the major obstacle to dislocation motion during creep, creep behavior of the steel is related to increase in subgrain width λ as a function of creep strain ε, namely *d*λ/*d*ε [22]. *d*λ/*d*ε is independent of creep test condition at high stresses. This fact results in the stress insensitive values of Ω at high stresses. In long-term creep at low stresses, *d*λ/*d*ε increases with decreasing stress, resulting in the increases in Ω at low stresses. The minimum creep rate is attained by dynamic balance between strain hardening (primary creep) and weakening due to the subgrain coarsening (tertiary creep). Another consequence of the increase in *d*λ/*d*ε is the decrease in ε_m with decreasing stress (see Fig.3 (a)). These stress dependences of Ω and ε_m are explained in more detail elsewhere [22].

EVALUATION OF RUPTURE LIFE

Equation (3) points out that creep strain goes up to very large value when t approaches $1/\beta$. Let us define an estimated rupture life t_r* as follows:

$$t_r^* = 1/\beta \tag{8}$$

An actual rupture life t_r can be shorter than t_r* since fracture occurs at a strain of around 20%. Necking and cavity formation in a specimen accelerate fracture during creep. The actual data points deviate downward from the linear relation of Eq.(2) as observed in Figs.2 and 4. This deviation can result in a rupture life longer than t_r*. Due to these uncertainties, a correlation of t_r* to t_r should be determined experimentally for accurate evaluation of rupture life. Creep curves of the four heats of Gr.91 steel were analyzed with Eq.(3). Obtained values of β are plotted against actual rupture life t_r in Fig.6. The following relation holds between t_r and β over the wide range of t_r from 44 to 96,000h:

$$t_r = t_o\,\beta^{-p} \tag{9}$$
$$t_o = 1.009, \quad p = 1.004$$

where t_o is a coefficient, and p is an exponent. The dotted lines in the figure represent a 99% confidence band. Width of the band corresponds to a factor of 1.12.

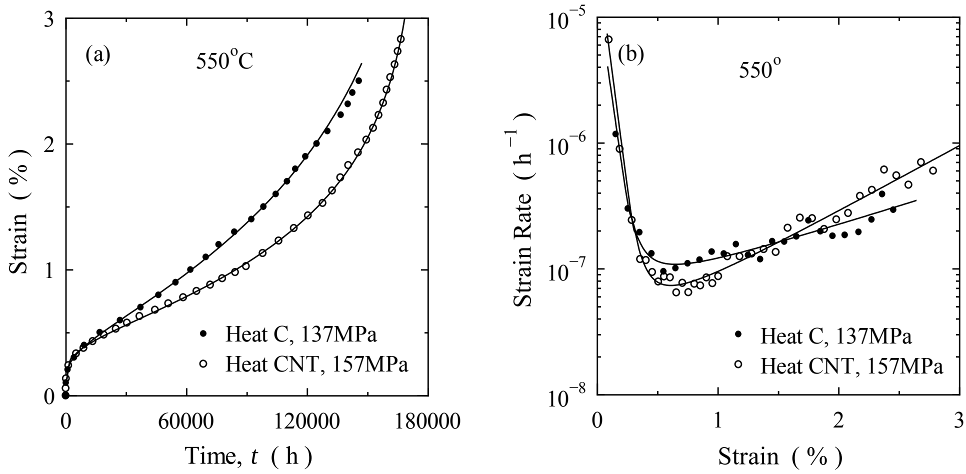

Figure 7: (a) On-going creep curves and (b) their strain rate vs. strain curves of heats C and CNT.

Two on-going creep curves are drawn in Fig.7 (a). The test durations elapsed are 145,700h and 166,600h for heats C and CNT, respectively. The corresponding strain rate vs. strain curves are drawn in Fig.7 (b). The strain at the minimum creep rate is less than 1% and the values of Ω are large (Ω = 70 in heat C and 120 in heat CNT). These are typical of creep curves tested in the long-term creep region. The solid curves drawn in Fig.7 are the results of the curve fitting based on Eq.(3). Good fit is achieved between the data points and the regression curves. The analyses provide the following values of t_r*:

$t_r^* = 1/\beta = 188{,}000$h at 137MPa, 550°C (Heat C)
$= 177{,}000$h at 157MPa, 550°C (Heat CNT)

Substitution of these values into Eq.(9) gives the following rupture lives:

$t_r = 199{,}000$h at 137MPa, 550°C (Heat C)
$= 188{,}000$h at 157MPa, 550°C (Heat CNT)

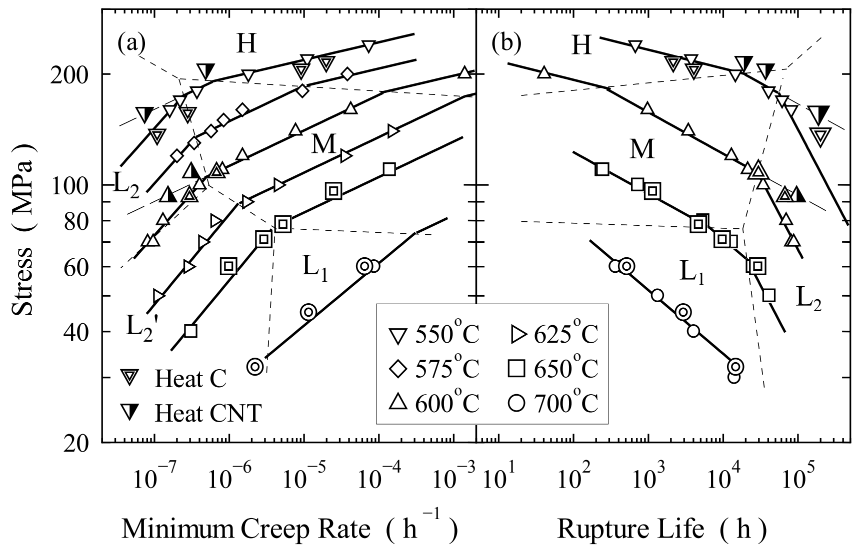

Figure 8: Stress dependence of (a) minimum creep rate and (b) rupture life of heats C (double symbols) and CNT (semi-solid symbols) together with those of heat MGC (open symbols). The solid lines are regression curves of heat MGC, and the dotted lines represent the boundaries between neighboring regions.

ASSESSMENT OF LONG-TERM CREEP BEHAVIOR

Minimum Creep Rate

Data points of heat MGC reported in NIMS Creep Data Sheet [23] are plotted against creep stress in Fig.8 with open symbols. Minimum creep rate $\dot{\varepsilon}_m$ is expressed as a function of stress σ and temperature T by the following equation:

$$\dot{\varepsilon}_m = \dot{\varepsilon}_o \sigma^n \exp(-Q/R\,T) \qquad (10)$$

where $\dot{\varepsilon}_o$ is a constant, n is the stress exponent, and Q is the activation energy. There are four regions with different values of stress exponent in Fig.8 (a); regions H, M, L_1 and L_2. Abe [10] analyzed the same data points of heat MGC but used the data points down to $\dot{\varepsilon}_m$ of $2x10^{-7}h^{-1}$ at 550°C, $4x10^{-7}h^{-1}$ at 600°C and $1.7x10^{-6}\,h^{-1}$ at 625°C. He has pointed out that there are two regions with n = 15 and 6. The present analysis uses all the data points of the heat down to $\dot{\varepsilon}_m$ of $1.6x10^{-7}h^{-1}$ at 550°C, $8x10^{-8}h^{-1}$ at 600°C and $1x10^{-7}h^{-1}$ at 625°C. The present analysis over the wilder range of creep rate finds another region L_2 with a low stress exponent in the low creep rate range. Stress exponents in the four regions are n = 21 in region H, 10 in region M, 6 in region L_1 and 4 in region L_2. In region L_2, Q = 350kJ/mol at temperatures from 550 to 600°C but 460kJ/mol between 625 and 650°C. Due to the difference in Q, region L_2 is divided further into L_2 (550 to 600°C) and L_2' (625 and 650°C). The solid lines in Fig.8 (a) are regression curves determined with Eq.(10) in each region of heat MGC. Region L_2 primarily corresponds to the low stress (long-term) region with large Ω and small ε_m. Region L_1 is also the low stress region. The creep temperature is fairly high and n takes the higher value of 6 in this region.

Data points of heats C and CNT of the present study are included in Fig.8 (a). Heats C and CNT were normalized at 1060°C for 60min contrary to 1050°C for 10min of heat MGC. The longer normalizing duration at the higher temperature gives larger grain sizes of heats C and CNT. The large grain size results in the lower creep rate of heat CNT [22]. Heat C was subjected to stress relief annealing for 500min at 740°C in addition to 60min tempering at 760°C. This long tempering makes a softer lath microstructure than that of heat MGC tempered for 30min at 765°C. Therefore, heat C has higher minimum creep rates than heat MGC at 550°C [22]. However, the creep rates of heats C and MGC are the same at 600°C and higher due to recovery of the initial lath microstructures.

The two data points of heat CNT at 600°C give stress exponent of about 4 typical of region L_2. The data points of heat C tested under 108 and 93MPa at 600°C are on the regression lines of heat MGC in region M and L_2, respectively. At 206MPa and 550°C $\dot{\varepsilon}_m$ of heat CNT is lower than that of heat MGC. On the other hand, the data point of heat CNT tested at 157MPa and 550°C is on the dashed line, which is an extension from region M of heat MGC. If region L_2 is absent in heat CNT, the minimum creep rate at 157MPa should be lower the dashed line. These findings indicate the presence of region L_2 in heat C and CNT. The value of $\dot{\varepsilon}_m$ of heat C tested at 137MPa and 550°C does not conflict with the presence of region L_2.

Rupture Life

Creep rupture data of Gr.91 steel have been published in NIMS Creep Data Sheet in 2014 [23]. Rupture data of a heat (MGC in the data sheet) are given in Fig.8 (b) with the open symbols. The regression lines drawn in the figure are results of a multi-region rupture data analysis reported in literature [3]. Data points tested at 575 and 625°C are removed for simplicity, but the whole data points are shown in the literature together with the regression lines. Heats C (double symbols) and CNT(semi-solid symbols) are the results of the present study. The data points at 137 (heat C) and 157MPa (heat CNT) crept at 550°C and at 108MPa (heat C) crept at 600°C were predicted by the analyses of on-going creep curves as explained in the previous section. The other data pointes of heats C and CNT were measured directly. There are the four regions H, M, L_1, and L_2 in the figure. Regions L_1 and L_2 primary correspond to the low stress region with large Ω and small ε_m. Rupture life t_r is represented by the following equation:

$$t_r = t_{ro}\, \sigma^{-n} \exp(Q/R\,T) \qquad (11)$$

where t_{ro} is a constant. Regions L_1 and L_2 are essentially the same in terms of creep damage mechanism, but n is greater in region L_1 probably due to the higher testing temperature. At 550°C the rupture lives are shorter in heat C and longer in heat CNT than those of heat MGC. These facts correspond to the ones found on the minimum creep rates in Fig.8 (a). At the other temperatures, heat C has the same rupture life as heat MGC in regions M and L_1, indicating almost disappearance of effects of the initial hardness on creep rupture life [22]. On the other hand, the rupture lives of both heats C and CNT are always longer in region L_2 than those of heat MGC due to their larger grain sizes [22]. These findings suggest different creep deformation and fracture mechanisms among regions H, M and L_2.

Let us examine the presence of region L_2 in heats C and CNT. The data point of heat C tested at 108MPa at 600°C is on the regression line of region M. If region L_2 is absent, the data point at 93MPa crept at 600°C should be on the extension from region M (dashed line), but takes a shorter rupture life than the extension. The data points of heat CNT at 216MPa and 206MPa crept at 550°C take longer rupture lives than the regression line of heat MGC (solid line). If region L_2 is absent, the data point of the heat tested at 157MPa and 550°C should have longer rupture life than the extension (dashed line) from region M. However, the data point is on the dashed line. The data points of heat C of 550°C tested at 216 and 206 MPa are slightly lower than the regression line. If region L_2 is absent, the data point of the heat tested at 137MPa and 550°C should be located at the same distance from the dashed line as those tested at 216 and 206MPa. However, the distance of the former is longer than the latter. All these findings are consistent with the presence of region L_2.

The data points of heats C and CNT at the low stresses in Fig.8 (a) indicate the presence of region L_2 with a low value of n in the heats. The data points of the heats at the low stresses in Fig.8 (b) also support the presence of region L_2. The creep curves tested in region L_2 (Figs.2 and 7) have the characteristics of the low stress creep, namely small strain to minimum creep rate and a large value of Ω. It follows from these facts that region L_2 appears in long-term range not only in heat MGC but also in hears C and CNT.

Region L_2 was found first in 2010 [16] and has been confirmed in 2016 [3], but is not recognized widely. However, the region is present in the present study. Service conditions of Gr.91 in power boilers and fast reactors, namely 10^5h at 600°C and $5x10^5$ h at 550°C, are in the region. We should pay more attention to the region L_2 for safe operation of plant components made of Gr.91 steel.

Summary

(1) Creep curves of Gr.91 steel can well be formulated with a creep curve equation based on the Ω creep curve equation, namely Eq.(3).
(2) Strain ε_m to minimum creep rate is about 2% at high stress, and decreases with decreasing stress at low stresses. The slope Ω of the asymptotic line in the tertiary creep is about 40 at high stresses, and increases to above 100 at low stresses. A small value of ε_m and large value of Ω is typical of long-term creep curves of the steel.
(3) Rupture life of the steel is very well correlated with the rate constant β in Eq.(3). Rupture life can be evaluated with the correlation (Eq.(9)), once β is determined by fitting of Eq.(3) to an on-going creep curve. This method enables rupture life evaluation of on-going creep before its fracture.
(4) The presence of long-term region L_2 is confirmed in heats C and CNT of the present study. Service conditions of plant components made of the steel are usually in the region. Stress exponents for minimum creep rate (n = 4) and for rupture life (n = 2.6) are low in the region. Creep curves in the region are characterized by a small value of ε_m (about 0.5%) and a large value of Ω (about 100).

Acknowledgements

The present study was supported by New Energy and Industrial Technology Development Organization (NEDO project # 1400070-0) and Japan Science and Technology Agency (ALCA project). This paper includes the result of "Technology development of fast breeder reactors, etc." entrusted to Japan Atomic Energy Agency (JAEA) by the Ministry of Economy, Trade and Industry (METI).

References

[1] Maruyama, K., and Yoshimi, K., "Influence of data analysis method and allowable stress criterion on allowable stress of Gr.122 heat resistant steel," *Trans. ASME, J. Press. Vess. Technol.*, Vol. 129 (2007), pp. 449-453.
[2] Maruyama, K., Nakamura, J., and Yoshimi, K., "Prediction of long-term creep rupture life of grade 122 steel by multiregion analysis," *Trans. ASME, J. Pressure Vessel Technol.*, Vol. 137, No. 2 (2015), pp. 021403-1-5.
[3] Maruyama, K., Nakamura, J., and Yoshimi, K., "Assessment of long-term creep rupture strength of T91 steel by multiregion rupture data analysis," *Trans. ASME, J. Pressure Vessel Technol.*, Vol. 138, No. 3 (2016), pp. 031407-1-9.
[4] Maruyama, K., Sawada, K., and Koike, J., "Strengthening mechanism of creep resistant tempered martensitic steel," *ISIJ Intern.*, Vol. 41 (2001), pp. 641-653.

[5] Abe, F., "Bainitic and martensitic creep-resistant steels," *Current Opinion in Solid State Mater. Sci.*, Vol. 8 (2004), pp. 305-311.
[6] Danielsen, H.K., and Hald, J., "Behaviour of Z phase in 9-12%Cr steels," *Energy Mater.*, Vol. 1 (2006), pp. 49-57.
[7] Maruyama, K., "Fracture mechanism map and fundamental aspects of creep fracture," Creep-resistant steels, Ed. By F. Abe, T. Kern, and R. Viswanathan, Woodhead Publishing (Cambridge, UK, 2008), pp. 350-364.
[8] Masuyama, F., "Advanced technology in creep life prediction and damage evaluation for creep strength enhanced ferritic steels," *Proceedings of high-temperature defect assessment-5*, Surry, UK, June 2010, CD-ROM.
[9] Kimura, K., and Takahashi, Y., "Evaluation of long-term creep strength of ASME grade 91, 92, and 122 type steels," *ASME 2012 Pressure Vessels and Piping Conference*, (2012), Paper No. PVP2012-78323.
[10] Abe, F., "Creep behavior, deformation mechanisms, and creep life of mod.9Cr-1Mo steel," *Metal. Mater. Trans.*, Vol. 46A, No. 12 (2015), pp. 5610-5625.
[11] Viswanathan, R., "Creep," Damage Mechanisms and Life Assessment of High Temperature Components, ASM Intern. (Metals Park, OH, 1989), pp. 59-110.
[12] Choudhary, B.K., "Tertiary creep behavior of 9Cr-1Mo steel," *Mater. Sci. Eng.*, Vol. 585A (2013), pp. 1-9.
[13] Prager, M., "Development of the MPC omega method for life assessment in the creep range," *Trans. ASME, J. Press. Vess. Technol.*, Vol. 117, No. 2 (1995), pp. 95-103.
[14] National Institute for Materials Science, "Creep deformation properties of 9Cr-1Mo-V-Nb steel tubes for boilers and heat exchangers and 9Cr-1Mo-V-Nb steel plate for boilers and pressure vessels," NIMS Creep Data Sheet, Atlas of Creep Deformation Property No. D-1, NIMS (Tsukuba, Japan, 2007), pp. 1-167.
[15] National Institute for Materials Science, "Creep deformation properties of 9Cr-1Mo-V-Nb steel plates for boilers and pressure vessels – effect of stress relieving heat treatment," NIMS Creep Data Sheet, Atlas of Creep Deformation Property No. D-2, NIMS (Tsukuba, Japan, 2008), pp. 1-159.
[16] Maruyama, K., Ghassemi Armaki, H., Chen, R.P., Yoshimi, K., Yoshizawa, M., and Igarashi, M., "Cr concentration dependence of overestimation of long term creep life in strength enhanced high Cr ferritic steels," *Int. J. Press. Vessels Pip.*, Vol. 87 (2010), pp. 276-281.
[17] Evans, R.W., Parker, J.D., and Wilshire, B., "An extrapolation procedure for long-term creep strain and creep life prediction with special reference to 1/2Cr1/2Mo1/4V ferritic steels", Recent Advance in Creep and Fracture of Engineering Materials and Structures, Ed. By B. Wilshire and D.R.J. Owen, Pineridge Press (Swansea, U.K., 1982), pp. 135-184.
[18] Maruyama, K., and Oikawa, H., "An extrapolation procedure of creep data for St determination: with special reference to Cr-Mo-V steel," *Trans. ASME, J. Press. Vess. Technol.*, Vol. 109, No. 1 (1987), pp.142-146.
[19] Maruyama, K., Nonaka, I., Sawada, K., Sato, H., Koike, J., and Umaki, H., "Improvement of omega method for creep life prediction," *ISIJ Intern.*, Vol. 37, No. 4 (1997), pp. 419-423.
[20] Abe, F., "Evolution of microstructure and acceleration of creep rate in tempered martensitic 9Cr-W steels," *Mater. Sci. Eng.*, Vol. A234-236 (1997), pp. 1045-1048.
[21] Dewees, D.J., and Hantz IV, B.F., "Review and development of primary load elevated temperature design rules," *ASME 2014 Pressure Vessels and Piping Conference*, (2014), Paper No. PVP2014-28797.
[22] Maruyama, K., Nakamura, J., and Yoshimi, K., to be published.
[23] National Institute for Materials Science, "Data sheets of the elevated-temperature properties of 9Cr-1Mo-V-Nb steel tubes for boilers and heat exchangers, 9Cr-1Mo-V-Nb steel plates for boilers and pressure vessels and 9Cr-1Mo-V-Nb seamless pipe for high temperature service," NIMS Creep Data Sheet No. 43A, NIMS (Tsukuba, Japan, 2014), pp. 1-71.